Nuclear Instruments and Methods in Physics Research A 1093 (2027) 171975

Contents lists available at ScienceDirect

Nuclear Inst. and Methods in Physics Research, A

journal homepage: www.elsevier.com/locate/nima

Full Length Article

Optimization of the FARICH technique for the SPD experiment☆

I.I. Anisimov [a,c], A.Yu. Barnyakov [a,b,*], V.S. Bobrovnikov [a,c], A.R. Buzykaev [a], A.V. Chepelev [a,b], R.A. Efremov [a,b], A.F. Danilyuk [d], A.A. Katcin [a,c], A.V. Kopotilov [e], E.P. Kovalev [d], A.Yu. Korzenev [g], E.A. Kravchenko [c,a], I.A. Kuyanov [a,b], A.D. Ofitserov [a,b], I.V. Ovtin [a,c], K.G. Petrukhin [a], A.Yu. Predein [d], S.A. Rozhkov [f], V.S. Rusetsky [e,f], D.K. Savenkov [a], V.S. Shvetsov [g]

[a] *Budker Institute of Nuclear Physics, Acad.Lavrentiev Prospect 11, 630090, Novosibirsk, Russia*
[b] *Novosibirsk State Technical University, Karl Marks Prospect 20, 630073, Novosibirsk, Russia*
[c] *Novosibirsk State University, Pirogova St. 1, 630090, Novosibirsk, Russia*
[d] *Boreskov Institute of Catalysis, Acad. Lavrentiev Prospect 5, 630090, Novosibirsk, Russia*
[e] *AO "Ekran FEP", Zelenaya gorka St. 1, 630060, Novosibirsk, Russia*
[f] *Rzhanov Institute of Semiconductor Physics, Acad. Lavrentiev Prospect 13, 630090, Novosibirsk, Russia*
[g] *Joint Institute of Nuclear Research, Joliot-Curie St. 13, 141980, Dubna, Russia*

ARTICLE INFO

Keywords:
Cherenkov radiation
Particle identification
MCP PMT
Aerogel
FARICH

ABSTRACT

A system of Cherenkov counters based on the FARICH (Focusing Aerogel RICH) technique is currently considered the main option for providing reliable π/K separation in the momentum range from 0.5 to 6 GeV/c for the SPD (Spin Physics Detector) experiment at the NICA (Nuclotron-based Ion Collider fAcility) collider, which achieved stable beam operation at the JINR (Dubna) for the first time in January 2026. Since 2004, the FARICH technique has been proposed for several high-energy physics (HEP) experiments and is now being optimized for the SPD experiment. The parameters of multilayer focusing aerogel radiators have been optimized. Several optimized aerogel samples were produced in 2025 and subsequently tested with relativistic electron beams. Beam test results are in good agreement with simulation results. The main ideas of the optimization and the beam test results are presented. As position-sensitive detectors for the SPD-FARICH system, square MCP (microchannel plate) based PMTs with multi-anode readout are being considered. The design of a photon detection module based on a square position-sensitive MCP PMT, to be manufactured in Russia, is described.

1. Introduction

Since 2004, R&D on RICH detectors based on focusing aerogel radiators (FARICH) has been conducted in Novosibirsk through a close collaboration between the Budker Institute of Nuclear Physics (BINP) and the Boreskov Institute of Catalysis (BIC) [1]. To achieve reliable π/K separation for momenta up to 6 GeV/c in the end-cap regions of the SPD experiment [2] at the Nuclotron-based Ion Collider fAcility (NICA) in Dubna, Russia, the FARICH detector was proposed in 2023 [3]. This proposal initially built upon numerous fruitful R&D results obtained in previous years for the FARICH system [4,5] of the Super C-τ Factory project in Russia [6,7] and the ARICH system of the Belle II experiment at KEK (Tsukuba, Japan) [8,9]. This work is devoted to the optimization of the FARICH technique for the SPD experiment conditions and requirements, and consists of: optimization of focusing aerogel radiators (Section 2); development of square position-sensitive MCP PMTs with appropriate front-end electronics (FEE) (Section 3); design of the FARICH system construction (Section 4).

The FARICH system will occupy two cylindrical gaps between the end-cap straw-tube trackers and the calorimeters, located at distances from 1506 to 1806 mm from the detector center along the beam axis, and spanning radii from 60 to 778 mm [2]. Given the expected bunch length of approximately $\sigma_z \approx 30$ cm [2], the system will detect particles within a pseudo-rapidity range of 1.3 to 4. The system will operate in an axial magnetic field of up to 1 T and in a radiation environment, which was evaluated using GEANT4 simulations (see Chapter 16 in [2]). According to these simulation results, the ionizing dose will not exceed several hundred grays per year of operation at the maximum interaction

☆ This article is part of a Special issue entitled: 'TIPP 2026' published in Nuclear Inst. and Methods in Physics Research, A.

* Corresponding author at: Budker Institute of Nuclear Physics, Acad.Lavrentiev Prospect 11, 630090, Novosibirsk, Russia.
E-mail address: A.Yu.Baryakov@inp.nsk.su (A.Yu. Barnyakov).

https://doi.org/10.1016/j.nima.2026.171975
Received 30 May 2026; Received in revised form 3 August 2026; Accepted 15 August 2026
Available online 22 August 2026

Table 1
Results of measured SPR, $L_{sc}^{400\ nm}$, N_{pe} and calculated N_σ for the different multilayer focusing aerogel samples.

Layers/n_{max}	Thickness, mm	$L_{sc}^{400\ nm}$, mm	Δ_{pix}, mm	SPR, mm	$\sigma_{\theta_c}^{1pe}$(exp), mrad	$\sigma_{\theta_c}^{1pe}$(sim) mrad	N_{pe}	N_σ at 6 GeV/c
4/1.046	35	62.5 ± 0.3	6	2.10 ± 0.005	10.0 ± 0.02	10.1	18.4 ± 0.05	4.25 ± 0.01
4/1.04	40	67.6 ± 0.9	6	2.36 ± 0.005	10.7 ± 0.02	10.8	16.7 ± 0.04	4.24 ± 0.01
3/1.04	40	64.2 ± 0.8	6	2.57 ± 0.005	11.6 ± 0.02	11.4	18.4 ± 0.04	4.10 ± 0.01

energy (27 GeV) and luminosity ($10^{32}\,cm^{-2}\,s^{-1}$), even in the inner tracking region.

The fluxes of non-ionizing particles, including photons, energetic (⩽10 keV), and thermal neutrons, were also calculated at several distinct points within the detector. Consequently, the flux in the region of the FARICH sensors and electronics plane can be estimated via interpolation as follows:

- photons – 5–20 × $10^2\,cm^{-2}\,s^{-1}$;
- thermal neutrons – 4–5 × $10^2\,cm^{-2}\,s^{-1}$;
- energetic neutrons – 3–15 × $10^2\,cm^{-2}\,s^{-1}$;
- charged particles – 2–100 × $10^2\,cm^{-2}\,s^{-1}$.

From these values, the neutron fluence per year of operation in the FARICH region can be estimated as 0.7–2 × $10^{10}\,n_{eq}/cm^2$. These estimates must be taken into account for the optimization of the FARICH system under the SPD experiment conditions.

2. Aerogel radiator optimization

Multilayer focusing aerogel optimization. In 2025, several multilayer focusing aerogel samples with varying configurations were manufactured in Novosibirsk. Their optical parameters were measured, and their focusing performance was tested using relativistic electrons at the BINP beam test facility [10]. The primary goal of this optimization is to identify the optimal technological approach for the mass production of aerogel focusing radiators without degrading the particle identification (PID) performance of the FARICH system. The following optimization approaches were investigated.

- To increase the separation of Cherenkov angles in the high-momentum range, the maximum refractive index was reduced from 1.05 to 1.04.
- To compensate for the resulting decrease in the number of detected photons per track, the total thickness of the tiles was increased from 35 mm to 40 mm.
- Furthermore, the thickness of each individual layer was increased, while the total number of layers was reduced from four to three. This adjustment is motivated by the fact that, with 6×6 mm^2 pixel size, the final Cherenkov angle resolution will be dominated by the spatial resolution of the photon detector.

It should be noted that a lower refractive index also reduces the Cherenkov ring radius. Consequently, the ratio σ_R/R increases, since the angular resolution is constrained by the spatial resolution of the photon detector. As a result, the particle separation capability deteriorates.

On the other hand, a smaller ring radius reduces the region of interest considered for Cherenkov ring reconstruction. This, in turn, decreases the number of fake hits originating from intrinsic noise of the photon detector and front-end electronics (FEE), thereby improving the stability of the reconstruction.

To determine the optimal trade-off, a full simulation of the FARICH system is required under realistic experimental conditions — either through hadron beam tests with actual photon detectors and FEE, or under full-ring detection conditions.

Table 1 presents a comparison of experimental results obtained for the different aerogel samples tested in the same conditions: 4 PMTs H12700 with pixel size (Δ_{pix}) 6 mm and focusing distance 200 mm. It includes data on the single photon resolution (SPR), the number of detected photons (N_{pe}), and the Rayleigh light scattering length at 400 nm ($L_{sc}^{400\,nm}$). The expected π/K separation power at a momentum of 6 GeV/c, expressed in terms of standard deviations (N_σ), is also presented in Table 1. The separation power is calculated according to the following equation:

$$N_\sigma = \frac{\Theta^\pi - \Theta^K}{\sigma_{\theta_c}^{1pe}/\sqrt{N_{pe}}}. \quad (1)$$

From Table 1, it can be seen that all tested aerogel samples are capable of providing reliable π/K separation for momenta up to 6 GeV/c. Also it is observed rather good agreement beam test results for single photon resolution $\left(\sigma_{\theta_c}^{1pe}(\mathrm{exp})\right)$ and simulation results $\left(\sigma_{\theta_c}^{1pe}(\mathrm{sim})\right)$.

All aerogel samples listed in Table 1 were tested with relativistic electrons at 2.5 GeV/c after annealing, which restored the aerogel's optical properties. Although the influence of adsorbed water on the SPR is negligible [11], annealing was performed to avoid potential effects from other substances adsorbed from the environment during the storage period. The same photon detector configuration was used for all samples, with a focusing distance of 200 mm from the entrance surface of the aerogel to the photon detector plane. In this configuration, the radii of the Cherenkov rings from the tested aerogels range from 45 (for n_{max} = 1.04) to 55 mm (for n_{max} = 1.046).

The focal distance of the multilayer aerogels is determined by the gradient of the refractive indices. For the tested samples, the differences between the maximum and minimum refractive indices are as follows:

- 1.046–1.039 for the 4-layer aerogel with a total thickness of 35 mm;
- 1.040–1.029 for the 4-layer aerogel with a total thickness of 40 mm;
- 1.040–1.030 for the 3-layer aerogel with a total thickness of 40 mm.

The real distribution of the refractive indices in the layers is controlled using a digital X-ray scanner, as described in [12,13]. The accuracy of such measurements is estimated as $\Delta n = \pm 0.001$. For all samples mentioned above, the refractive indices in the layers are in good agreement with the initial specifications, within the measurement accuracy. The measured values of the refractive index correspond to a wavelength of 400 nm.

The dispersion of the refractive index in Novosibirsk aerogel was measured by two different groups, in 2007 [14] and in 2015 [15]. According to these measurements, it does not exceed $\frac{\Delta n}{n} \leqslant 10^{-3}$ in the optical wavelength range. This implies that the accuracy of our refractive index measurements using the X-ray scanner is of the same order as the refractive index dispersion, and its contribution to the overall SPR can be estimated via simulation as approximately 1 mrad in quadrature.

The effects of refractive index deviations from the calculated profiles were also investigated using simulations. It was shown that there are no focusing issues if the refractive indices are consistently higher or lower by the same amount. However, the focusing effect is significantly degraded if the refractive indices are increased in some layers and decreased in others simultaneously.

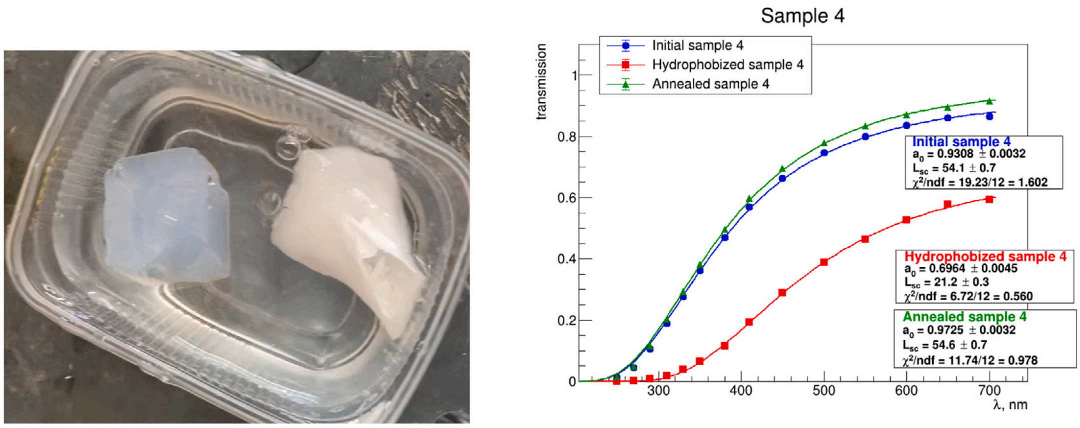

Fig. 1. Aerogel hydrophobization: (left) comparison of hydrophilic and hydrophobic Novosibirsk aerogels reacted with water; (right) transparency spectra of Novosibirsk aerogel before hydrophobization, after hydrophobization, and after restorative baking.

Aerogel hydrophobization. The first experiments on hydrophobization of aerogel produced in Novosibirsk were carried out in the fall of 2025 and early 2026. It was shown that this process decreases aerogel transparency; however, this effect is reversible. That is, it is possible to restore the aerogel transparency by baking it at a high temperature (approximately 400–500°C) for 4–6 h.

Fig. 1 demonstrates the effects of aerogel hydrophobization: the left image compares the reactions of hydrophilic and hydrophobic Novosibirsk aerogels with water, while the right plot presents the measured wavelength dependence of transparency for an aerogel sample before hydrophobization, after hydrophobization, and after restorative baking.

Thus, hydrophobization will allow us to produce thick focusing aerogel samples using standard technology, then render them hydrophobic, shape and cut them as needed (e.g., using a water-jet cutting machine) without concern for their optical parameters. After all manipulations, the initial transparency can be restored before the start of the experiment. Further R&D on optimizing hydrophobization procedures is currently ongoing.

3. Development of the square MCP PMT

Since the FARICH system will be placed in the end-cap regions of the SPD experiment, the direction of the magnetic field allows two candidates for position-sensitive photon detectors to be considered: MCP PMTs and SiPM arrays. However, SiPMs have two significant disadvantages — namely, high dark count rates and strong sensitivity to neutron fluence — which prevent their use as photon detectors for Cherenkov counters in any real colliding beam experiment. According to preliminary estimations for the FARICH system in the SPD experiment, the neutron fluence will increase the intrinsic noise of the SiPMs by a factor of two per year of operation (see Section 1 and paper [16]). Therefore, MCP PMTs emerge as strong candidates for the photon detector.

In 2025, a new design for a photon detection module based on a square MCP PMT was developed for production through a collaboration between the Budker Institute of Nuclear Physics (BINP) and its industrial partner, CJSC "Ekran FEP" [17]. Fig. 2 shows a view of the square MCP PMT with a 16 × 16 array of 2.8×2.8 mm pixels and the FEE block. The overall dimensions of the module are 59×59×79.5 mm. It consists of three main parts:

- a metal–ceramic housing of the square MCP PMT with 256 square anodes (2.8 × 2.8 mm each);
- front-end readout electronics mounted on four PCBs (printed circuit boards), which are connected to the anode plane via flexible PCBs;
- a shield made of carbon fiber reinforced plastic and a joining board designed to hold all parts together and enable the assembly of photon detection module arrays.

The baseline option for the photocathode (PC) of these MCP PMTs is a multialkali PC with extended UV sensitivity, deposited on a fused quartz input window. According to simulation results, this type of PC increases the detection efficiency of Cherenkov photons by a factor of 1.5 compared to traditional multialkali PCs. Some results of the measured quantum efficiency for the new type of PC, along with a comparison to traditional ones, can be found in Ref. [5].

The parameters of the FARICH detector, based on different PC options (UV-extended and standard multialkali), were evaluated from simulations performed within the GEANT4 framework and are presented in Table 2. As the radiator, the 4-layer aerogel with $n_{max} = 1.046$ and a total thickness of 35 mm, presented in Table 1, was used. As photon detectors, an array of square position-sensitive MCP PMTs with lateral dimensions of 33×33 mm and 8 × 8 pixels, each of size 3×3 mm, as described in [5], was implemented in the simulation. From Table 2, it can be seen that aerogel dispersion in the UV region increases the SPR by 0.3 mrad, while the number of detected photons increases by a factor of 1.45 and the Cherenkov angle resolution improves by 13%. Additional improvement is expected from the increased geometrical efficiency of the square MCP PMT with lateral dimensions of 59×59 mm, as well as from enhanced photoelectron collection efficiency achieved by coating the MCP surfaces using ALD (Atomic Layer Deposition) technology. We expect that ALD applied to the internal surfaces of the channels will help improve the lifetime of the PCs, while ALD on the input surface of the MCP will also increase collection efficiency by capturing photoelectrons that would otherwise be recoiled from the flat MCP surface. According to our preliminary tests and estimations, this approach can increase the photoelectron collection efficiency by 20%, though it may degrade the time resolution from 30–50 ps (obtained for MCPs without additional coating of the input surface) to 200–300 ps. Detailed results of these investigations will be published later. For the SPD project, excellent time resolution of the FARICH system is not considered a critical parameter, as a dedicated time-of-flight system is foreseen for PID in the low-momentum range.

4. FARICH system construction design

Taking into account the results presented in the previous sections, the conceptual design of the FARICH system for the SPD experiment was developed. A sketch of the system is presented in Fig. 3. The aerogel plane consists of 69 tiles shaped as round disk sectors, arranged in four radial segments from an inner radius of 60 mm to an outer

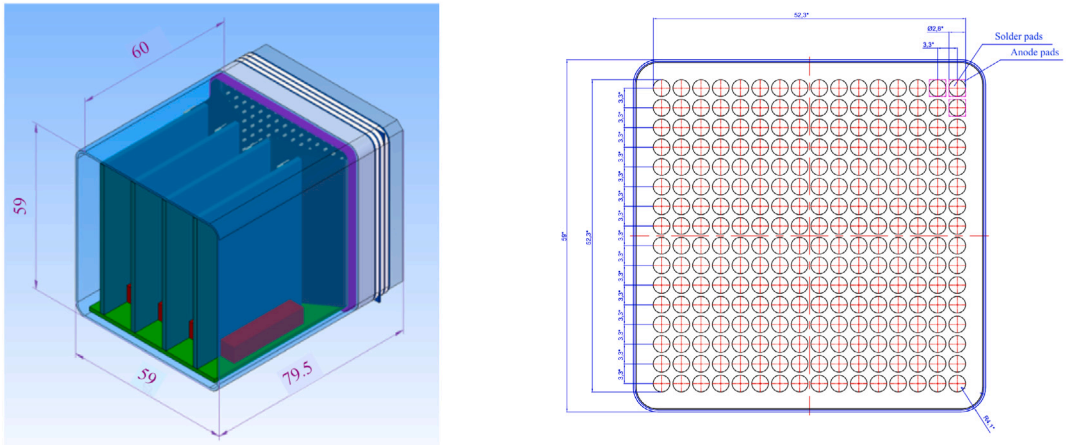

Fig. 2. Conceptual design of the square MCP PMT for the FARICH system of the SPD experiment: 3D model view from the FEE side (left); sketch of the anode plane (right).

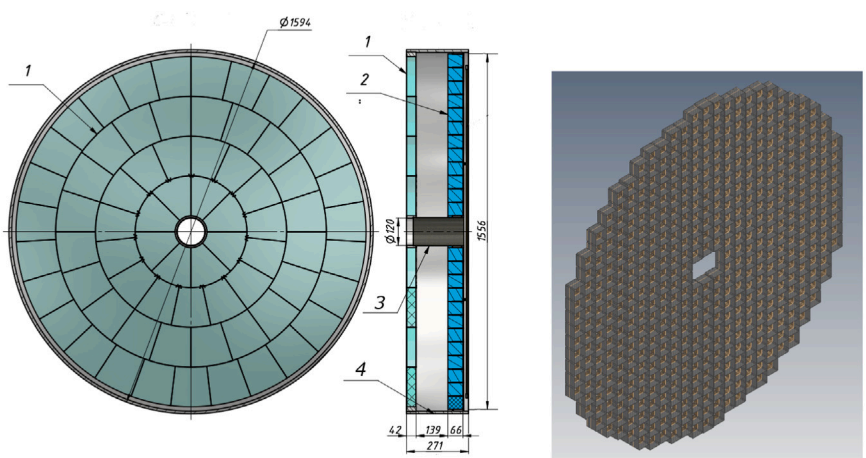

Fig. 3. Design of the FARICH subsystem for the SPD experiment: schematic view of the system with key components labeled: 1 – aerogel layout; 2 – photon detection modules; 3 – inner shell; 4 – outer shell (left); 3D view of the support grid for the photon detection modules (right).

Table 2
Main parameters of the FARICH options based on different photocathode types.

	Standard multi-alkali (Std.)	UV-extended (UV)	UV vs. Std.
$\sigma_{\theta_c}^{1pe}$, mrad	6.77 $\pm$ 0.01	7.04 $\pm$ 0.02	$7.04/6.77 = 1.040 \pm 0.003$
$N_{pe}(\beta = 1)$	8.83 $\pm$ 0.02	12.84 $\pm$ 0.01	$12.84/8.83 = 1.450 \pm 0.003$
$\sigma_{\theta_c}^{track}$, mrad	2.278 $\pm$ 0.002	1.965 $\pm$ 0.002	$1.965/2.278 = 0.863 \pm 0.001$

radius of 778 mm. The system occupies a distance of 271 mm along the beam line.

Fig. 3(right) shows the grid used to arrange the photon detection plane, which consists of 508 photon detection modules based on square MCP PMTs. The grid is made of Carbon Fiber Reinforced Plastic (CFRP) with a wall thickness of 0.3 mm. Deformation calculations show that the expected load (the weight of one module is approximately 400 g) will result in a maximum deformation of the CFRP grid of no more than 6 μm.

5. Summary

The FARICH detector is the baseline option for particle identification (PID) in the end-cap regions of the SPD experiment. Several configurations of focusing multilayer aerogels were manufactured and tested in 2025. Beam test results with relativistic electrons at the BINP are very promising and demonstrate that all new aerogel types are capable of providing excellent π/K separation over the operational momentum range from 0.5 to 6 GeV/c.

In 2025, a new design for a square MCP PMT-based photon detection module for RICH detectors was developed in Novosibirsk. The production of the first prototype of the module is expected soon. Furthermore, the first version of the technical design of the FARICH subsystem for the SPD experiment has been developed.

Declaration of competing interest

The authors declare that they have no known competing financial interests or personal relationships that could have appeared to influence the work reported in this paper.

References

[1] A. Yu Barnyakov, et al., NIM A 553 (2005) 70.
[2] SPD Collaboration, V. Abazov, et al., Nat. Sci. Rev. 1 (2024) 1.

[3] Alexander Yu Barnyakov, et al., Phys. Part. Nucl. 56 (2025) 3, 652–655.
[4] Alexander Yu Barnyakov, et al., Internat. J. Modern Phys. A 39 (2024) 26n27, 2442012.
[5] Ivan Igorevich Anisimov, et al., JUSTC 55 (12) (2025) 1206, (5pp).
[6] Super Charm Tau Factory, SCT Collab, Conceptual design report part one (physics program, detector), 2018, https://sct.inp.nsk.su/media/cdr/sct_cdr_vol_1.pdf.
[7] M.N. Achasov, et al., Phys. Uspekhi 67 (1) (2024) 55–70.
[8] T. Iijima, et al., NIM A 548 (2005) 383.
[9] S. Iwata, et al., Prog. Theor. Exp. Phys. 502 (2016) 033H01.
[10] G.N. Abramov, et al., JINST 11 (2016) P03004.
[11] A. Yu Barnyakov, et al., Nucl. Instrum. Meth. A 598 (2009) 166–168.
[12] E.A. Babichev, et al., NIM A 513 (2003) 57.
[13] A. Yu Barnyakov, et al., NIM A 766 (2014) 235.
[14] T. Bellunato, et al., Eur. Phys. J. C 52 (2007) 759?764.
[15] M. Contalbrigo, CLAS12 RICH Project Mid-Term Review: Aerogel, JLab, 2015, https://www.fe.infn.it/u/mcontalb/JLAB12/RICH_midterm/Contalbrigo_Aerogel.pdf.
[16] M. Calvi, et al., NIM A 922 (2019) 243.
[17] https://ekranfep.ru/ru/.